High-Performance Integrated ZnO Nanowire UV Sensors on Rigid and Flexible Substrates

Suo Bai, Weiwei Wu, Yong Qin, Nuanyang Cui, Dylan J. Bayerl, and Xudong Wang**

Due to the large surface area-to-volume ratio and high quality crystal structure, single nanowire (NW)-based UV sensors exhibit very high on/off ratios between photoresponse current and dark current. Practical applications require a large-scale and low-cost integration, compatibility to flexible electronics, as well as reasonably high photoresponse current that can be detected without high-precision measurement systems. In this paper, NW-based UV sensors were fabricated in large-scale by integrating multiple NWs connected in parallel via the contact printing method. Linear scaling of the photoresponse current with the number of NWs is demonstrated. Integrated ZnO NW UV sensors were fabricated on rigid glass and flexible polyester (PET) substrates at the macroscopic scale. The flexible and rigid sensors performed comparably, exhibiting on/off current ratios approximately three orders of magnitude higher than sensors made from polycrystalline ZnO thin films. Under UV irradiance of 4.5 mW cm^{-2} and 3 V bias, photoresponse currents and on/off current ratios for the rigid and flexible UV sensors reached 12.22 mA and 82 000, and 14.1 mA and 120 000, respectively. This result suggests that lateral integration of semiconductor NWs is an effective approach to large-scale fabrication of flexible NW sensors that inherit the merits of single-NW-based systems with unaffected performance compared to using rigid substrate.

1. Introduction

During the last two decades, one-dimensional (1D) nanostructures have attracted great interests due to their outstanding properties and potential applications.[1–4] Zinc oxide (ZnO), one of the most important metal oxides, has a wide bandgap of 3.37 eV and high exciton binding energy of 60 meV at room temperature. The nanowires (NWs) morphology is considered a promising building block for light emitting diodes,[5] sensors,[6] solar cells,[7] electromechanical transducers[8] and piezotronics.[9] For photodetector applications, high on/off current ratio, fast response and recovery, and large photoresponse current are desirable sensor characteristics.[10] ZnO NWs have show great promises for UV sensors because of their high on/off current ratio,[11] fast response and recovery,[12] visible light blind, low-cost fabrication[13–15] and potential for flexible electronics.[16] However, an essential hindrance to ZnO single-NW UV sensors is the very low photoresponse current due to the small size of individual NWs. High-precision measurement systems are necessary to detect the signal, making such sensors cost prohibitive. Many methods to enhance UV photoresponse current have been investigated. Surface functionalization and CdTe decorations were demonstrated to increase the photoresponse current of ZnO single-NW UV sensors.[10,17] Ultra-long bridging ZnO NWs were used to improve UV sensor performance.[18] The most straightforward and cost-effective way to increase the photoresponse current is to connect multiple ZnO NWs in parallel, which also preserves the performance merits of single-crystalline NWs.[19] Contact printing method has been shown as an effective approach to assemble horizontal NW arrays on flat substrate surfaces.[20–22] The horizontal NW arrays are considered more suitable for large-scale device integration, particularly for flexible electronics, compared to other arrangements of NWs, such as vertically aligned arrays. A number of promising applications have been demonstrated using horizontal NW arrays, such as transistor arrays,[20,21] sensors,[22,23] transparent electrodes,[24,25] energy harvesters,[26] and so forth.

In this paper, NW-based UV sensors were fabricated in large-scale by integrating multiple NWs connected in parallel via the contact printing method. A linear monotonically increasing relationship between the photoresponse current of ZnO NW UV sensors and the number of NWs connected in parallel was demonstrated. Integrated ZnO NW UV sensors were fabricated on rigid glass and flexible polyester (PET) substrates at macroscopic scale. The flexible sensors exhibited comparable performance to those fabricated on rigid glass substrates, which generated enhanced UV photoresponse currents at the milliampere (mA) level. On/off current ratios of the integrated ZnO NW UV sensors were three orders of magnitude higher than those of UV sensors made from polycrystalline ZnO thin films. The

Dr. S. Bai, Dr. W. W. Wu, Prof. Y. Qin, Mr. N. Cui
Institute of Nanoscience and Nanotechnology
Lanzhou University
Gansu 730000, China
E-mail: qinyong@lzu.edu.cn
Mr. D. J. Bayerl, Prof. X. D. Wang
Department of Materials Science and Engineering
University of Wisconsin at Madison
Madison, Wisconsin 53706, USA
E-mail: xudong@engr.wisc.edu

DOI: 10.1002/adfm.201101319

parallel NW integration method demonstrated here is a direct conversion of vertical ZnO NWs into horizontal arrays, which is more versatile and simpler compared to crystal lattice-directed horizontal growth[27] or pattern-confined growth techniques.[28] It could be an effective approach to fabrication of flexible NW-based sensors with largely enhanced performance.

2. Integration of Multiple ZnO NWs in UV Sensors.

The UV photoresponse current (ΔI) is defined as: $\Delta I = I - I_0$, where I_0 is the dark current and I is the photoresponse current under UV illumination. For a UV sensor composed of multiple NWs connected in parallel, the photoresponse current would linearly increase with the number of NWs: $\Delta I = \Sigma(I - I_0)$. Meanwhile, the high UV on/off current ratio of single-NW-based sensors will be maintained. This principle was first demonstrated by characterizing and comparing the performance of single-NW UV sensors with Ohmic electrode contacts (inset of **Figure 1**a) and their parallel integrations (Figure 1a). Different photoresponse currents from the individual single-NW sensors were likely due to the geometric differences of the ZnO NW building blocks. Generally, enhanced photoresponse currents from parallelly integrated NW sensors were observed. The increment was found to be ~70% of the sum of the photoresponse currents of individual sensors. This discrepancy may relate to the variable performance of individual single-NW sensors and the enlarged contact resistance when integrated together. Nevertheless, this experiment confirmed that the response of single-NW UV sensors can be effectively enhanced by integrating multiple NWs in parallel.

Additional experiments were conducted on a larger number of NWs with uniform geometry and physical property. The side-branches of ZnO microcombs were used as NW building blocks for fabricating multi-NW UV sensors. SEM image showed that the NW branches had a relatively uniform length (±1.4%) and diameter (±10%) (inset of Figure 1b). In addition, the NW branches on the same ZnO micorcomb were grown at the same time and under the same condition, which insured their physical properties were uniform. Therefore, the microcombs are good candidates to test sensor performance without influence from NW nonuniformities. The microcomb-based multi-NW UV sensors were fabricated by depositing stripes of silver (Ag) thin film electrodes at the root and the tip of the branches (Figure S1) to form Ohmic contacts (Figure 1b). In this configuration, the branches of the microcomb can be considered as individual NWs connected in parallel. The original number of NWs was counted as 219. To investigate the dependence of UV photoresponse on number of NWs, the photoresponse current was measured after selectively removing NWs from the device. Higher UV photoresponse currents were generated with larger numbers of NWs (Figure 1c). Peak photoresponse currents were plotted as a function of the number of NWs connected in parallel (Figure 1d). A linear regression was applied to the data with a coefficient of determination R^2 value of 0.94, indicating a linear relationship between photoresponse current and number of uniform NWs connected in parallel.

The recovery time (τ), defined as the time for the photoresponse current to drop to 1/e (37%) of the maximum photoresponse current,[29] was further investigated and compared. The microcomb-based multi-NW UV sensors exhibited a τ of ~24 s; while the single-NW UV sensor with Ohmic contacts had an average τ of 14 s. The comparable recovery times evidence that integration of multiple NWs together would not significantly alter other performance features of single-NW based sensors.

The same series of experiments was conducted on multi-NW UV sensors with Schottky electrode contact. Implementing Schottky contact is believed to increase the on/off current ratio and shorten the response and recovery time,[30] since the strong local electric field at the reverse-biased Schottky barrier can rapidly separate the photon-generated electrons and holes.[31] Multi-NW UV sensors were fabricated by integrating several NWs in parallel with a palladium (Pd) electrode for Schottky contact (inset of Figure 1e). Maximum photoresponse current increased linearly from 5 nA to 0.45 μA as the amount of NWs increased from 1 to 13. This result indicates that the photoresponse current enhancement effect was independent of the type of electrode connection. The τ value was found to be ~0.9 s for the Schottky-type multi-NW UV sensor (Figure 1f), which was 30 times faster than that of Ohmic-type UV sensors. Therefore, based on above experiment results, it can be concluded that integration of multiple NWs in parallel could effectively enhance photoresponse current while maintaining other merits of single-NW-based UV sensors.

3. Large-Scale Fabrication of Integrated NW UV Sensors

Study of the multi-NW integration for UV sensors paved the way for scaling NW-based sensor systems from microscopic to macroscopic. In this section, we describe the fabrication and characterization of macroscale integrated NW UV sensors.

First, vertically aligned ZnO NW arrays were grown on a silicon (Si) substrate by chemical vapor deposition (CVD) (**Figure 2**a). These NWs were 30 μm long and 450 nm wide. Then, a thin film of polydimethylsiloxane (PDMS) was spin-coated onto a glass substrate and gently pressed onto the vertical ZnO NW arrays. A slight lateral shifting of the glass substrate transferred ZnO NWs to the PDMS surface with the orientation well aligned with the shifting direction (Figure 2b). Another UV-transparent glass substrate with Ag interdigitated transducer (IDT)-type electrodes was pressed onto the ZnO NW-coated PDMS surface, completing the integrated NW UV sensor (Figure 2c). Owing to the parallel alignment of ZnO NWs, we need only align the electrode pattern with the NW orientation to connect all NWs in parallel between the electrodes, as shown in Figure 2d. This approach conveniently separated electrode patterning from NW alignment processes, significantly simplifying fabrication. By patterning multiple different electrode designs on the substrate, this approach can be extended to realize large-scale NW sensor arrays.

Pressing the Ag electrodes directly onto the aligned ZnO NWs provided an Ohmic contact as shown in **Figure 3**a.

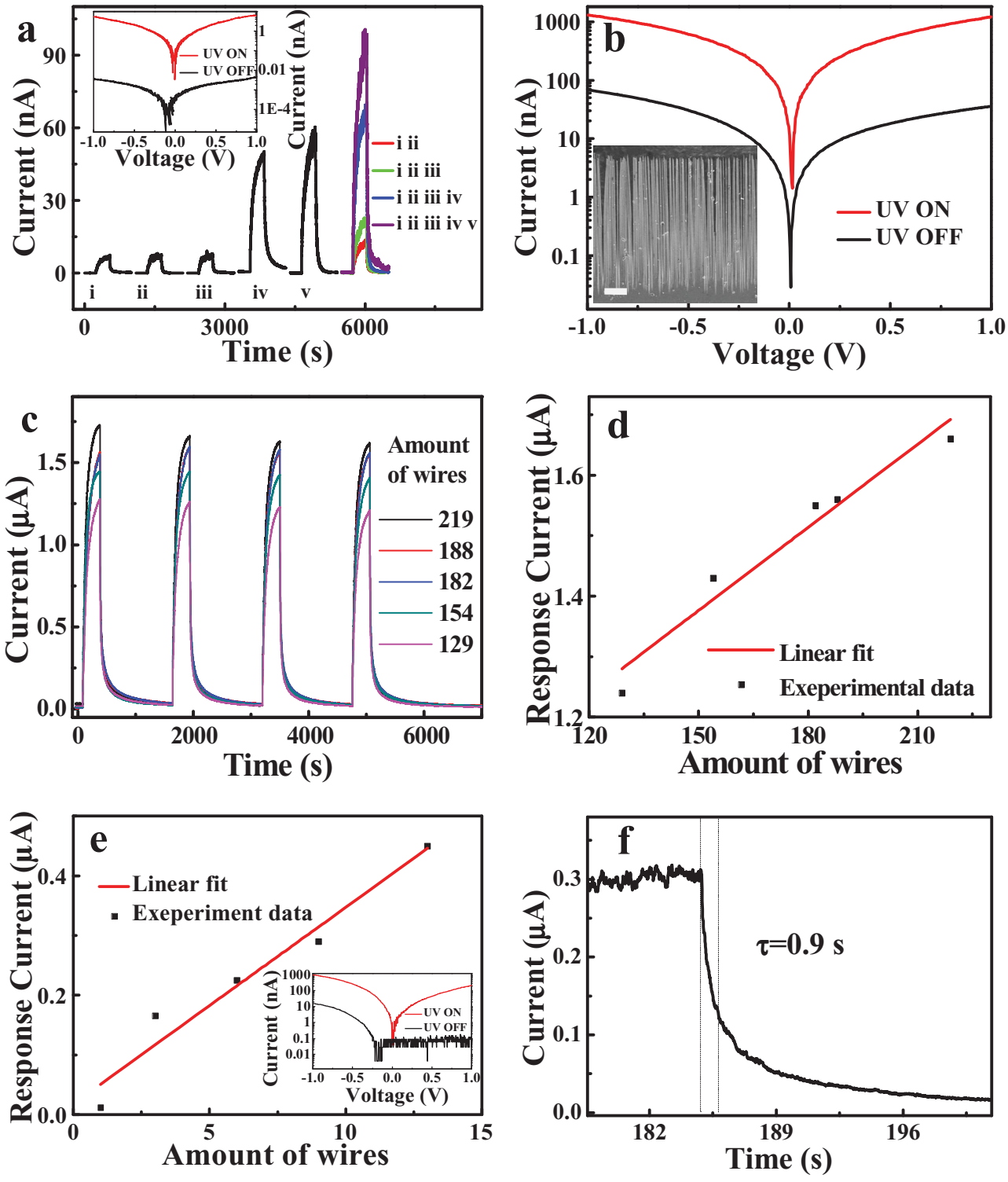

Figure 1. a) UV photoresponse of five different UV sensors made from single ZnO NWs and the corresponding UV responses when connecting them in parallel. Inset is the IV curve of sample i with/without UV illumination showing Ohmic contact. b) IV curves of a microcomb-based sensor with/without UV illumination. Inset is an SEM image of ZnO microcomb and the scale bar is 20 μm. c) Photoresponse under 4.5 mW cm^{-2} of UV irradiance and bias voltage of 1 V with different numbers of NWs connected in parallel. d) Plot of the maxium photoresponse current versus the number of NWs connected in parallel. e) Plot of the maxium photoresponse current versus the number of NWs connected in parallel with Schottky contacts. Inset is IV curve with/without UV illumination showing Schottky contact. f) Recovery current curve of a Schottky contact multi-microwire UV sensor after UV irradiance of 4.5 mW cm^{-2}.

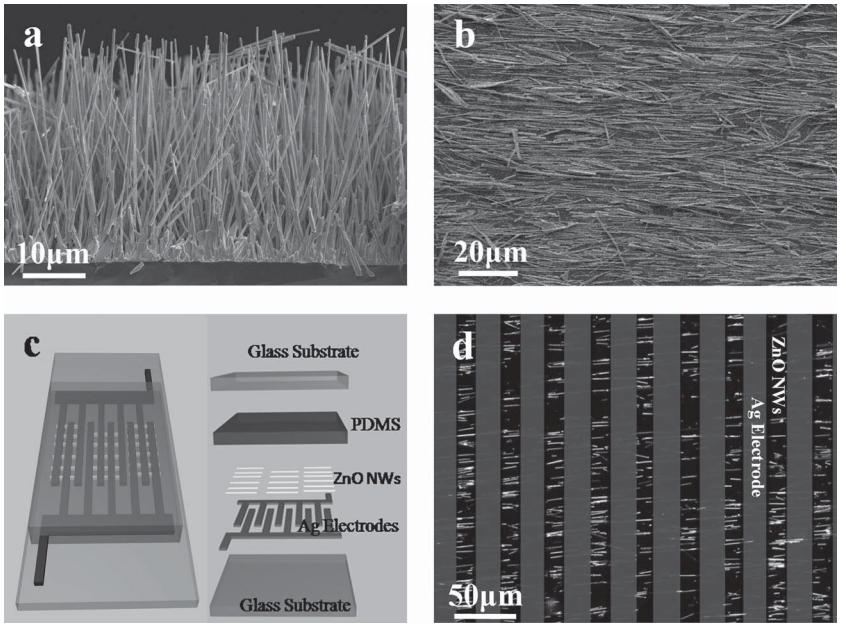

Figure 2. a) SEM image of a vertical ZnO NW array grown on Si substrate. b) Parallel-aligned ZnO NW layer on the surface of a PDMS film. c) Schematic design of a integrated NW UV sensor. d) Optical microscope dark field image of ZnO NWs connected in parallel between Ag electrodes.

Characterization of time-resolved photoresponse of the integrated NW UV sensor under UV irradiance of 4.5 mW cm^{-2} and applied bias of 1 V showed a maximum photoresponse current of 1.08 mA (Figure 3b). The photoresponse current increased to 12.22 mA when 3 V bias was applied (Figure S2), which was large enough to be detected by a passive mechanical ammeter.

The on/off current ratio of the integrated NW UV sensor was measured to be 83000 at 1 V bias and 82000 at 3 V bias under 4.5 mW cm^{-2} of UV irradiance. These values are one order of magnitude larger than that of a single-NW UV sensor (~6000), which demonstrates sensing merits beyond photoresponse current by the integrated NW design.

UV photoresponse current of the integrated NW sensor under a wide range of UV illumination intensity at 1 V bias are shown in Figure 3c. Lower currents were detected at weaker irradiances. The lowest detectable UV irradiance was ~100 nW cm^{-2}, with a peak photoresponse current of ~100 nA (inset of Figure 3d) and an on/off current ratio of 12. Based on this sensing response, we believe the integrated NW UV sensor can detect even weaker UV light. However, the detection limit of our UV detector precluded calibrating irradiances below 100 nW cm^{-2}. The peak photoresponse current at each UV irradiance level was plotted in Figure 3d. The observed gradual saturation of photoresponse current at higher UV irradiances is consistent with the performance of single ZnO NW-based UV detector. One possible reason is the limited number of available surface-adsorbed oxygen-electron pairs (O_2^-) that could enhance photoresponse current by trapping photon-generated holes.[32]

One significant merit of the integrated NW UV sensor is that the functional sensor elements are equivalently single-crystalline ZnO retaining the associated performance advantages, though they are composed of millions of NWs. Therefore, this technique lends itself well to a large-scale, bottom-up, low-cost fabrication approach to realizing performance superior to conventional polycrystalline thin film devices. In order to validate this statement, we fabricated a polycrystalline ZnO thin film-based UV sensor with the same area dimensions as the integrated NW UV sensor. This sensor was composed of a 500 nm-thick ZnO thin film sputtered on a 1×2.6 cm^2 area of a glass substrate and covered with identical Ag IDT-electrodes for Ohmic contacts (Figure S3a). Photoresponse of this device was characterized by the same measurement procedures. From time-resolved UV photoresponse measurement under UV irradiance of 4.5 mW cm^{-2} and 1 V bias (Figure S3b), the on/off current ratio was only 62 (3 orders of magnitude smaller than integrated NW sensors) and the recovery time τ was 5750 s (400 times slower than the NW-based

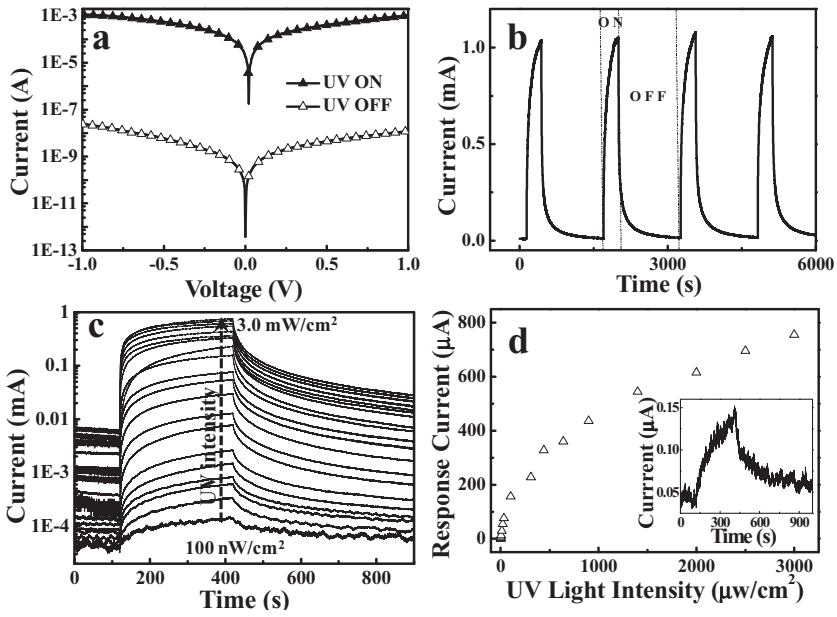

Figure 3. a) IV curves of the integrated NW UV sensor with and without UV illumination. b) Photoresponse of the integrated NW UV sensor under UV irradiance of 4.5 mW cm^{-2} and bias voltage of 1 V. c) Photoresponse of the integrated NW UV sensor under various UV illumination intensities at a bias voltage of 1 V. d) Plot of the maxium photoresponse current versus UV illumination intensity with 1 V bias. Inset is the photoresponse under UV irradiance of 100 nW cm^{-2}.

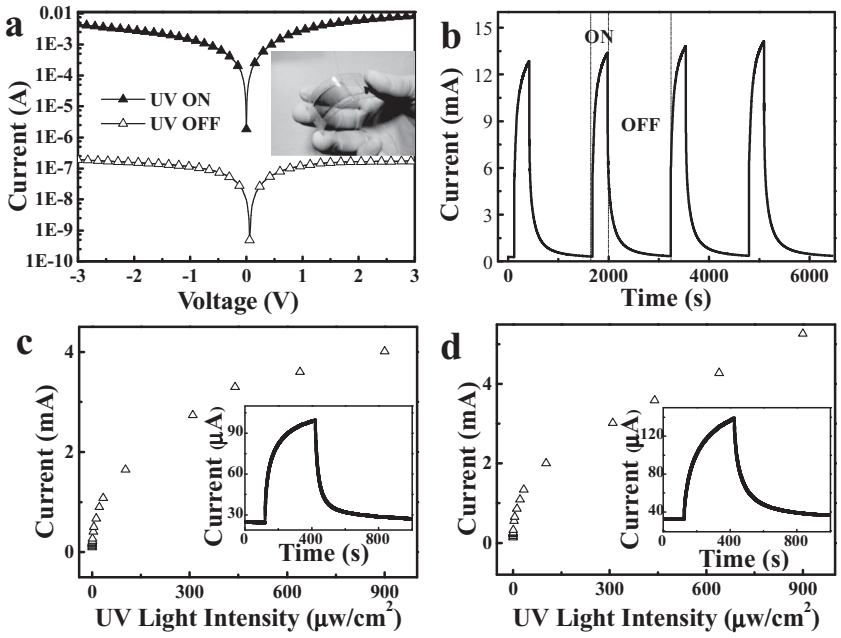

Figure 4. a) IV curves of the flexible UV sensor with and without UV illumination. Inset is a photo of a flexible integrated NW UV sensor. b) Time-dependent photoresponse of the flexible UV sensor at a bias voltage of 3 V under UV irradiance of 4.5 mW cm^{-2}. c) and d) are the plots of the maxium photoresponse current versus the UV illumination intensity with 3 V bias when the sensor is relaxed or deflected, respectively. Insets are the corresponding photoresponse under UV irradiance of 100 nW cm^{-2}.

sensors). The superior on/off current ratio and recovery time of the integrated NW UV sensors over the polycrystalline thin film UV sensor can be attributed to the high specific surface area and single-crystalline character of the NW building blocks.

4. Flexible Integrated NW UV Sensors

Our fabrication technique can be directly applied to flexible polymer substrates by replacing the glass substrates with a PET film. A flexible integrated NW UV sensor was thus realized, as shown in the inset of **Figure 4**a. Ohmic contact between the Ag electrodes and the ZnO NWs on the PET substrate was confirmed by IV measurements (Figure 4a). Time-resolved UV photoresponse measurements under UV irradiance of 4.5 mW cm^{-2} and 3 V bias (Figure 4b) showed a very high photoresponse current of 14.1 mA. The on/off current ratio was calculated to be 120000 (the dark current of this sensor is ~110 nA), exceeding even that of the integrated ZnO NW UV sensors on rigid glass substrates. Peak photoresponse current under different UV irradiances are shown in Figure 4c and the corresponding time-dependent current curves are included in Figure S4. The flexible UV sensor exhibited the same photocurrent-UV irradiance relationship as the sensors built on glass substrates. At the lowest calibrated UV irradiance (100 nW cm^{-2}), the flexible UV sensor showed a high on/off current ratio of ~870 (inset of Figure 4c), implying the ability to sense weaker UV light.[18,33,34]

The performance of the flexible UV sensor was also characterized when bent to a curvature of 25 m^{-1}. Comparing photoresponse currents of the sensor when bent (Figure 4d) to the unbent situation (Figure 4c) showed that UV detection capability was well preserved under deflection. Under weak UV irradiance of 100 nW cm^{-2}, the deflected flexible sensor exhibited an on/off current ratio of 1094, as shown in the insert in Figure 4d. Under 4.5 mW cm^{-2} of UV irradiance, the on/off current ratio increased to 110000 (the dark current is ~120 nA). The nearly unchanged performance of the flexible UV sensor under deflection demonstrates another advantage over single-crystalline thin film based devices, where strain would be a significant issue that impacts the performance.[35] Since our integrated NW design structurally discontinued the functional sensor elements (the NWs), bending-induced strain was most likely concentrated at the boundaries between adjacent NWs and at NW-electrode interfaces, instead of within the body of NWs. Device deflection thus has little impact on single-crystalline NW sensing elements, resulting in the observed near-invariance of sensor performance under flexure.

5. Conclusions

In summary, we demonstrated a bottom-up approach to fabricating macroscopic integrated ZnO NW UV sensors. Well-controlled experiments demonstrated a linear increasing relationship between photoresponse current and the number of NWs connected in parallel. Macroscopic multi-NW-based UV sensors were fabricated by transferring vertically aligned ZnO NWs to a parallel-aligned layer on a PDMS surface, followed by integration with electrodes patterned on rigid glass substrates and flexible PET substrates. This multi-NW sensor design retained all the merits of single-NW devices, including high on/off current ratio and fast response and recovery times. It also offered several unique advantages over single-NW and thin film devices: 1) significant enhancement of photoresponse current due to the large number of NWs integrated into the sensor design; 2) the fabrication approach is easily scalable to manufacture large area NW-based sensor arrays; 3) the device can be integrated with plastic substrates to achieve a flexible UV sensor; 4) the approach is low-cost and bottom-up, yet offers performance orders of magnitudes higher than polycrystalline thin films devices. In addition, the flexible integrated NW UV sensor response was nearly unaffected under deflection, suggesting an alternative strategy to design flexible electronics that incorporate the high performance of single-crystalline building blocks but with minimal impact from bending-induced strain.

6. Experimental Section

Fabrication of ZnO NWs and Microcombs: Vertically aligned ZnO NW arrays were synthesized on (100) Si substrate with a standard double-tube CVD system. The detailed experimental setup can be found in

ref [19]. In short, the mixture of ZnO (0.81 g) and graphite (C) (0.12 g) is placed at the sealed end of a small quartz tube. A clean Si substrate is put 20 cm from the mixture in the gas flow direction. The furnace is heated to 1050 °C at a rate of 50 °C/minute with Ar and O_2 flowing. ZnO NW arrays were grown during heating at 1050 °C for 1.5 hours. The ZnO microcomb structure was synthesized using a vacuum tube-based CVD system. ZnO (3 g) and C (3 g) were mixed and heated to 1100 °C at ramping rate 20 °C/minute. The system was kept at this temperature for 40 minutes. Ar (90 sccm) and O_2 (10 sccm) were used as carrier and reaction gases, bringing the vacuum of the deposition system to ~270 Pa. The ZnO microcombs were formed on and collected from an Al_2O_3 substrate located 0.5 cm downstream from the source material.

Fabrication of Integrated NW UV Sensors: A 300 μm thick layer of PDMS was spin-coated on a glass substrate with a rotation speed of 1000 rpm. The cured PDMS layer was then gently pressed on the ZnO NW arrays and slowly rubbed across. The sticky PDMS surface pulled NWs away from the Si substrate and aligned them in parallel to the moving direction of the substrate. Then, Ag or Pd IDT-electrodes were fabricated on another glass substrate through a standard photolithograph process. Finally, the glass substrate with electrodes was pressed onto the parallel-aligned ZnO NW layer on the PDMS/glass substrate. The two glass substrates were fixed together using acrylate glue. For fabrication of the flexible UV sensor, PET films were used instead of glass and glass/PDMS substrates and the device fabrication process was otherwise unchanged.

UV Sensor Characterization: IV curve and dark current measurements were performed using DS345 30 MHz synthesized function generator and SR 570 low-noise current preamplifier. A UV detector (Photoelectric Instrument Factory of Beijing Normal University, UV-A) was used to quantify UV irradiance. During measurement, the NW UV sensor was initially shielded from UV exposure, allowing only the UV detector to be exposed. After recording UV irradiance incident on the commercial detector, the NW UV sensor was uncovered and the response was measured. After 5 minutes of exposure, the sensor was shielded again and allowed to recover for 21 minutes. These procedures were repeated over a range of UV light irradiances from 100 nW cm^{-2} to 3 mW cm^{-2}.

Supporting Information

Supporting Information is available from the Wiley Online Library or from the author.

Acknowledgements

S. Bai, W. W. Wu, and Y. Qin contributed equally to this work. Research was supported by NSFC (NO. 50972053), NCET (NO. NCET-08), Ph.D. Programs Foundation of Ministry of Education of China (NO. 20090211110026), the Fundamental Research Funds for the Central Universities (No. lzujbky-2010-k01), Special Talent Funding of Lanzhou University, NSF(DMR-0905914) and UW graduate school. We also thank Mr. L. Meng for helping with synthesizing ZnO NW samples.

Received: June 9, 2011
Published online:

[1] S. Iijima, *Nature* **1991**, *354*, 56.
[2] B. Tian, T. J. Kempa, C. M. Lieber, *Chem. Soc. Rev.* **2009**, *38*, 16.
[3] C. M. Lieber, Z. L. Wang, *Mrs Bulletin* **2007**, *32*, 99.
[4] F. Patolsky, G. F. Zheng, C. M. Lieber, *Anal. Chem.* **2006**, *78*, 4260.
[5] A. Tsukazaki, A. Ohtomo, T. Onuma, M. Ohtani, T. Makino, M. Sumiya, K. Ohtani, S. F. Chichibu, S. Fuke, Y. Segawa, H. Ohno, H. Koinuma, M. Kawasaki, *Nat. Mater.* **2005**, *4*, 42.
[6] Q. Wan, Q. H. Li, Y. J. Chen, T. H. Wang, X. L. He, J. P. Li, C. L. Lin, *Appl. Phys. Lett.* **2004**, *84*, 3654.
[7] M. Law, L. E. Greene, J. C. Johnson, R. Saykally, P. D. Yang, *Nat. Mater.* **2005**, *4*, 455.
[8] Z. L. Wang, J. H. Song, *Science* **2006**, *312*, 242.
[9] Z. L. Wang, *Adv. Funct. Mater.* **2008**, *18*, 3553.
[10] L. Luo, Y. F. Zhang, S. S. Mao, L. W. Lin, *Sensor. Actuat. A-Phys.* **2006**, *127*, 201.
[11] C. S. Lao, M. C. Park, Q. Kuang, Y. L. Deng, A. K. Sood, D. L. Polla, Z. L. Wang, *J. Am. Chem. Soc.* **2007**, *129*, 12096.
[12] A. Trinchi, K. Galatsis, W. Wlodarski, Y. X. Li, *IEEE Sens. J.* **2003**, *3*, 548.
[13] P. D. Yang, H. Q. Yan, S. Mao, R. Russo, J. Johnson, R. Saykally, N. Morris, J. Pham, R. R. He, H. J. Choi, *Adv. Funct. Mater.* **2002**, *12*, 323.
[14] L. E. Greene, M. Law, J. Goldberger, F. Kim, J. C. Johnson, Y. F. Zhang, R. J. Saykally, P. D. Yang, *Angew. Chem. Int. Edit* **2003**, *42*, 3031.
[15] Y. Qin, R. S. Yang, Z. L. Wang, *J. Phys. Chem. C* **2008**, *112*, 18734.
[16] S. Y. Ju, A. Facchetti, Y. Xuan, J. Liu, F. Ishikawa, P. D. Ye, C. W. Zhou, T. J. Marks, D. B. Janes, *Nat. Nanotechnol.* **2007**, *2*, 378.
[17] R. S. Aga, D. Jowhar, A. Ueda, Z. Pan, W. E. Collins, R. Mu, K. D. Singer, J. Shen, *Appl. Phys. Lett.* **2007**, *91*, 232108.
[18] Y. B. Li, F. Della Valle, M. Simonnet, I. Yamada, J. J. Delaunay, *Nanotechnology* **2009**, *20*, 045501.
[19] W. Wu, S. Bai, N. Cui, F. Ma, Z. Wei, Y. Qin, E. Xie, *Sci. Adv. Mater.* **2010**, *2*, 402.
[20] J. H. Ahn, H. S. Kim, K. J. Lee, S. Jeon, S. J. Kang, Y. G. Sun, R. G. Nuzzo, J. A. Rogers, *Science* **2006**, *314*, 1754.
[21] A. Javey, S. Nam, R. S. Friedman, H. Yan, C. M. Lieber, *Nano Lett.* **2007**, *7*, 773.
[22] Z. Y. Fan, J. C. Ho, Z. A. Jacobson, H. Razavi, A. Javey, *P. Natl. Acad. Sci. USA* **2008**, *105*, 11066.
[23] P. C. Chen, S. Sukcharoenchoke, K. Ryu, L. G. de Arco, A. Badmaev, C. Wang, C. W. Zhou, *Adv. Mater.* **2010**, *22*, 1900.
[24] A. R. Madaria, A. Kumar, F. N. Ishikawa, C. W. Zhou, *Nano Res.* **2010**, *3*, 564.
[25] S. De, T. M. Higgins, P. E. Lyons, E. M. Doherty, P. N. Nirmalraj, W. J. Blau, J. J. Boland, J. N. Coleman, *Acs Nano* **2009**, *3*, 1767.
[26] G. A. Zhu, R. S. Yang, S. H. Wang, Z. L. Wang, *Nano Lett.* **2010**, *10*, 3151.
[27] B. Nikoobakht, A. Herzing, *Acs Nano* **2010**, *4*, 5877.
[28] S. Xu, Y. Ding, Y. G. Wei, H. Fang, Y. Shen, A. K. Sood, D. L. Polla, Z. L. Wang, *J. Am. Chem. Soc.* **2009**, *131*, 6670.
[29] J. B. K. Law, J. T. L. Thong, *Appl. Phys. Lett.* **2006**, *88*, 133114.
[30] J. Zhou, Y. D. Gu, Y. F. Hu, W. J. Mai, P. H. Yeh, G. Bao, A. K. Sood, D. L. Polla, Z. L. Wang, *Appl. Phys. Lett.* **2009**, *94*, 191103.
[31] Y. F. Hu, J. Zhou, P. H. Yeh, Z. Li, T. Y. Wei, Z. L. Wang, *Adv. Mater.* **2010**, *22*, 3327.
[32] C. Soci, A. Zhang, B. Xiang, S. A. Dayeh, D. P. R. Aplin, J. Park, X. Y. Bao, Y. H. Lo, D. Wang, *Nano Lett.* **2007**, *7*, 1003.
[33] A. J. Gimenez, J. M. Yanez-Limon, J. M. Seminario, *J. Phys. Chem. C* **2011**, *115*, 282.
[34] T. Zhai, L. Li, X. Wang, X. S. Fang, Y. Bando, D. Golberg, *Adv. Funct. Mater.* **2010**, *20*, 4233.
[35] M. J. Liu, H. K. Kim, *Appl. Phys. Lett.* **2004**, *84*, 173.